ACS APPLIED MATERIALS & INTERFACES

Research Article

www.acsami.org

Passivation of Aluminum Nanoparticles by Plasma-Enhanced Chemical Vapor Deposition for Energetic Nanomaterials

Anaram Shahravan,[†] Tapan Desai,[‡] and Themis Matsoukas*[,†]

[†]Department of Chemical Engineering, The Pennsylvania State University, University Park, Pennsylvania 16802, United States

[‡]Advanced Cooling Technologies, Inc., Lancaster, Pennsylvania 17601, United States

Supporting Information

ABSTRACT: We have produced passivating coatings on 80-nm aluminum particles by plasma-enhanced chemical vapor deposition (PECVD). Three organic precursors—isopropyl alcohol, toluene, and perfluorodecalin—were used to fabricate thin films with thicknesses ranging from 5 nm to 30 nm. The coated samples and one untreated sample were exposed to 85% humidity at 25 °C for two months, and the active Al content was determined by thermogravimetric analysis (TGA) in the presence of oxygen. The results were compared with an uncoated sample stored in a glovebox under argon for the same period. We find that all three coatings provide protection against humidity, compared to the control, and their efficacy ranks in the following order: isopropyl alcohol < toluene < perfluorodecalin. This order also correlates with increasing water contact angle of the three solid coatings. The amount of heat released in the oxidation, measured by differential scanning calorimetry (DSC), was found to increase in the same order. Perfluorodecalin resulted in providing the best protection, and it produced the maximum enthalpy of combustion, $\Delta H = 4.65$ kJ/g. This value is higher than that of uncoated aluminum stored in the glovebox, indicating that the coatings promote more complete oxidation of the core. Overall, we conclude that the plasma polymer coatings of this study are suitable passivating thin film for aluminum nanoparticles by providing protection against oxidation while facilitating the complete oxidation of the metallic core at elevated temperature.

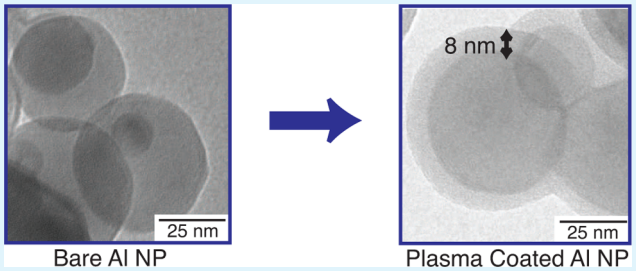

KEYWORDS: *aluminum nanoparticle, passivation, plasma polymer, nanoenergetic, functionalization, PECVD*

1. INTRODUCTION

High-performance energetic materials (e.g., explosives, rocket fuels) are designed to store large amounts of chemical energy with the ability to release it instantly on demand. Metal particles are prime candidates as additives to energetic materials, because they oxidize readily and release large amounts of heat.[1−3] Aluminum particles are currently being used in solid rocket booster fuels,[4] but a major drawback is their low rate of energy release, compared to other carbon-based energetic compounds, e.g., TNT, HMX, and RDX.[5] Several approaches have been developed to overcome this limitation and improve the rate of oxidation.[6] One strategy is to utilize very fine particles (<100 nm in size).[1,6−8] In addition to exhibiting higher rate of oxidation, small particles oxidize more completely, unlike micrometer-sized particles, whose oxidation is eventually arrested by the formation of a thick oxide layer.[9] This layer offers natural protection of the inner metallic core[10−12] but also adds dead weight. For particles in the nanometer range, this can be a serious problem. For example, for a particle 40 nm in diameter, the oxide layer (typically ∼4 nm) occupies 50% of the total mass of the nanoparticle. This has led to various other methods to passivate the particle surface to protect against oxidation or other contamination of the metal.[13−15]

The ideal coating should enhance nanoparticle properties. It should protect the metal from oxidation and other contamination and increase the rate of energy release at elevated temperatures. Noble metals and metal oxides[5,16] have been shown to provide protection for the aluminum core, as well as enhanced energy content, because of intermetallic reactions between the coatings and the core.[10] Boron has been used to stabilize aluminum propellants[17,18] by providing desirable surface characteristics, such as high corrosion resistance.[17,19] Carbon offers similar protection at low temperature and is stable at elevated temperatures.[20] More elaborate surface modifications involve in situ surface functionalization of freshly synthesized (oxide-free) aluminum nanoparticles using compounds, such as perfluoroalkyl carboxylic acids ($C_{13}F_{27}COOH$), formic acid, and aldehydes.[21−24] Some organic materials have been also used to stabilize aluminum nanoparticles, including waxes, ethanol, and fluoropolymer,[17] but the coatings were found to be permeable to oxygen and thus lacking in their capacity to provide passivation. Here, we report on a different approach that utilizes plasma-enhanced chemical vapor deposition (PECVD) to produce a surface coating of

Received: March 2, 2014
Accepted: April 30, 2014
Published: April 30, 2014

   dx.doi.org/10.1021/am5012707 | ACS Appl. Mater. Interfaces 2014, 6, 7942−7947

controllable thickness that provides superior passivation against environmental oxygen and moisture during storage but also enhances the energetic content of the particles.

Plasma-deposited solids have unique properties that are especially advantageous as passivating barriers for nanoenergetic materials. Most notably, plasma polymers produce hydrophobic surfaces.[25−28] Hydrophobicity adds a chemical interaction to the physical barrier, which alone cannot provide satisfactory protection against moisture.[17,29] Plasma deposited solids are chemically inert and thermally stable up to 250 °C.[30,31] They contain elements of their precursor molecules, typically carbon, oxygen, and fluorine.[32−35] These elements oxidize readily under combustion conditions, thereby exposing the aluminum core, and they may also contribute to the overall enthalpy of reaction.[25] As a dry gas-phase process, plasma offers a further advantage of a well-controlled environment. Unlike liquid phase processing, which exposes particles to a complex reaction medium and requires drying and additional separation steps to recover the particles, plasma reaction occurs in an inert environment. The deposition process is flexible and can be applied to any solid substrate, including metallic[36] and nonmetallic materials.[37−40] A broad choice of organic precursors may be used, including hydrocarbons, alcohols, and fluorocarbons, which offers a degree of flexibility in controlling the interfacial properties of the film.[41] Finally, the process provides very good control of the thickness of the coatings, which is a linear function of the deposition time.[39]

2. MATERIALS AND METHODS

Aluminum nanoparticles (99.9+%, 80 nm) with particle diameters in the narrow range of 80−100 nm were purchased from Nanostructured and Amorphous Materials, Inc. Nanoparticles were incubated in a desiccator under an inert atmosphere. They were transferred from their original container into small vials and stored in a glovebox under argon until time to use. Three organic precursors were used in this study: isopropyl alcohol (IPA 99.5% obtained from VWR), toluene (EMD chemicals), and perfluorodecalin (PFD 99% VWR).

The setup for the deposition process is shown in Figure 1. It consists of four main systems: the precursor delivery system; a

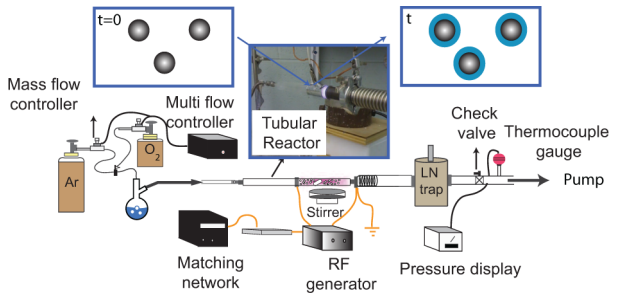

Figure 1. Schematic of the plasma deposition process illustrating the precursor delivery system, vacuum and pressure controllers, glass reactor, and radio-frequency (RF) generator.

tubular reactor, where the deposition process takes place; vacuum pumps, with the associated pressure controllers; and a radio frequency (RF) generator equipped with a matching box. Prior to the deposition process, 10 mL of the organic precursor was measured and poured into a glass flask connected to the reactor via a vacuum pipe. The temperature of this flask was maintained constant at 35 °C for isopropyl alcohol and perfluorodecalin, and at 45 °C for toluene. The glass flask is a bubbler for vapor delivery, with one inlet connected to an argon gas cylinder equipped with a gas flow controller. Argon at a constant flow rate (6 sccm) is mixed in the bubbler with organic vapor (0.5 sccm) and is led into the reactor. Immediately before connecting the reactor to the pump, the aluminum nanoparticles are transferred to the reactor using a metallic spatula. To promote uniform exposure of particles to the plasma, a small magnetic stirrer is placed inside the glass reactor that shakes particles during the reaction. The tubular glass tube is connected to the pump with a vacuum pipe connected to the tube with an O-ring and a clamp. After tightening the clamp, the check valve between the pump and the reactor is gradually opened to begin evacuation. When the reactor pressure reaches 200 mTorr, the RF power is turned on. The plasma is formed by two external electrodes, separated 1 in. from each other, one of which is connected to the RF source while the other is grounded. The plasma is operated at 30 W when IPA or PFD are the precursors, and at 40 W when toluene is used. The power is higher when toluene is used to avoid the formation of particles, which tend to form at lower power.[31] During deposition, a small magnetic plate is placed underneath the reactor and is set at 100 rpm to agitate the nanoparticles. A liquid nitrogen trap with a cool wall is used to condense any organic vapors escaping the reactor before entering the pump. At the end of the experiment, particles are collected from the reactor wall and are placed in the desiccator, where they are stored for further characterizations.

The thickness of the coating was measured by transmission electron microscopy (TEM), using a Philips Model (FEI) EM420T system. The morphology of the coatings and the effect of exposure to moisture was also studied by field-emission scanning electron microscopy (FESEM) (Leo, Model 1530). Micrographs of aluminum wafers were collected by scanning electron microscopy (SEM) (Hitachi, Model S-3500N) equipped with a diffraction energy microscopy (EDS). Thermogravimetric analysis (TGA) and differential scanning calorimetry (DSC) were performed on a TA Instruments Model SDT 2960 system equipped with a simultaneous differential scanning calorimetry−thermogravimetric analysis (DSC-TGA) system that operates under an air flow of 40 mL/min.

3. RESULTS AND DISCUSSION

Three precursors were used in this study: isopropyl alcohol (IPA), perfluorodecalin (PFD), and toluene. TEM micrographs confirm the formation of smooth solid coatings from all three precursors. The coatings appear as a lightly shaded layer surrounding darker particles (Figure 2). It is radially conformal to the particle and shows good adhesion to the surface. The thickness of the film is a linear function of time, ∼1 nm/min for all precursors,[30] and provides a means for controlling the thickness of the coatings. For the samples shown in Figure 2 the deposition time was 30 min for IPA, 10 min for PFD, and 7 min for toluene resulting in 30 ± 5, 10 ± 2, and 7 ± 2 nm coatings, respectively. In all of the subsequent experiments, the thickness of the coating is 5 nm.

A unique characteristic of plasma deposition of hydrocarbon-based solid is the water-repellent properties of the surface.[41] Figure 3 shows measurements of the sessile water droplet contact angle conducted on flat silicon wafers coated by the three precursors under conditions identical to those for coating particles. Plasma-polymerized IPA is the most hydrophilic of

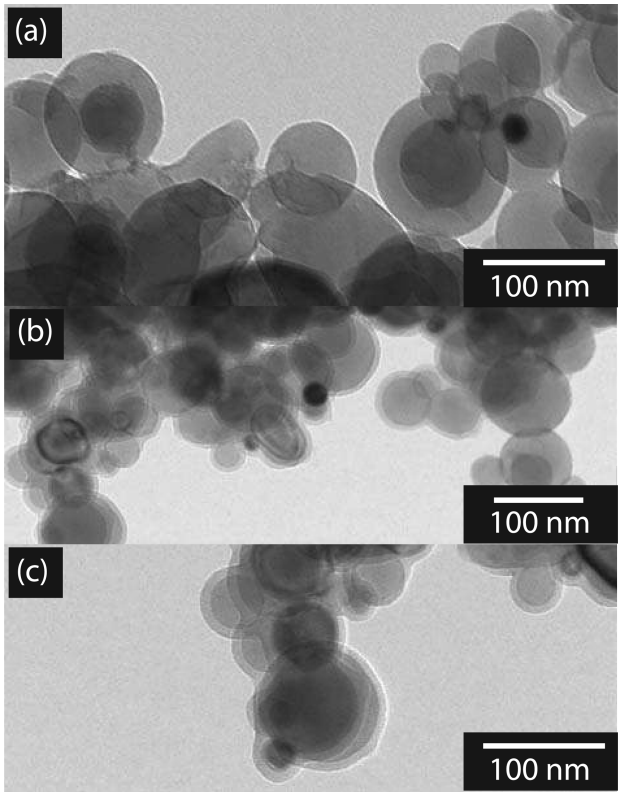

Figure 2. Transmission electron microscopy (TEM) micrographs of aluminum particles coated with (a) isopropyl alcohol, (b) toluene, and (c) perfluorodecalin plasma polymer.

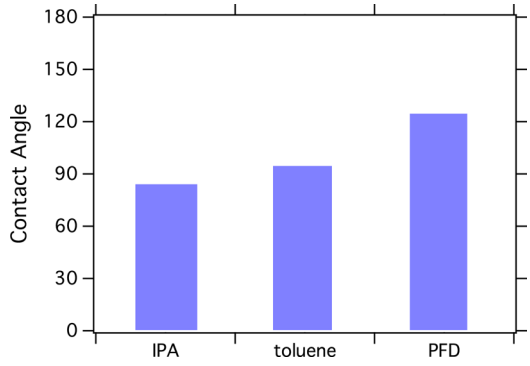

Figure 3. Water contact angle measurements of coated silicon wafer with isopropyl alcohol (IPA), toluene, and perfluorodecalin (PFD).

the three coatings, with a contact angle of 84° ± 2°. As we reported previously,[30] IPA coatings show good affinity for water and particles coated using this precursor can form stable aqueous dispersions. Toluene and PFD films are increasingly more hydrophobic with contact angles of 92° ± 2° and 125°, respectively. Particles coated with these two materials cannot be dispersed in water. The water-repelling properties of the coatings suggest that these materials may offer enhanced protection to the aluminum surface. As a first test, we examined the stability of coated aluminum wafers with PFD plasma polymer against exposure to sodium hydroxide (NaOH). For these experiments, a drop of 0.5 M NaOH was placed on three aluminum wafers, one coated with PFD. As a control, an uncoated wafer also was tested. The native aluminum surface, shown in Figure 4a, is smooth with some waves and marks that were formed during the polishing process. After exposure to

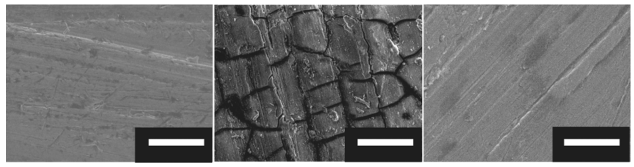

Figure 4. SEM images of (a) an uncoated aluminum wafer, (b) an uncoated aluminum wafer exposed to NaOH, and (c) and a coated aluminum with PFD plasma polymer, which is exposed to NaOH. Scale bar = 1 μm.

NaOH for 5 h, the uncoated surface shows significant damage (Figure 4b). The PFD-coated surface, on the other hand, shows no visible damage and its appearance is indistinguishable from that of the unexposed surface (Figure 4c). These experiments were repeated three times. SEM images show similar results.

We now proceed to characterize the ability of plasma-deposited coatings to protect aluminum nanoparticles against a humid atmosphere. A sample of uncoated aluminum and three samples of coated nanoparticles with each precursor were kept in a closed container under 85% relative humidity at 25 ± 5 °C for two months. As a control, we also examined a sample of uncoated nanoparticles stored in the glovebox during this period. These particles are seen in Figure 5a, which reveals

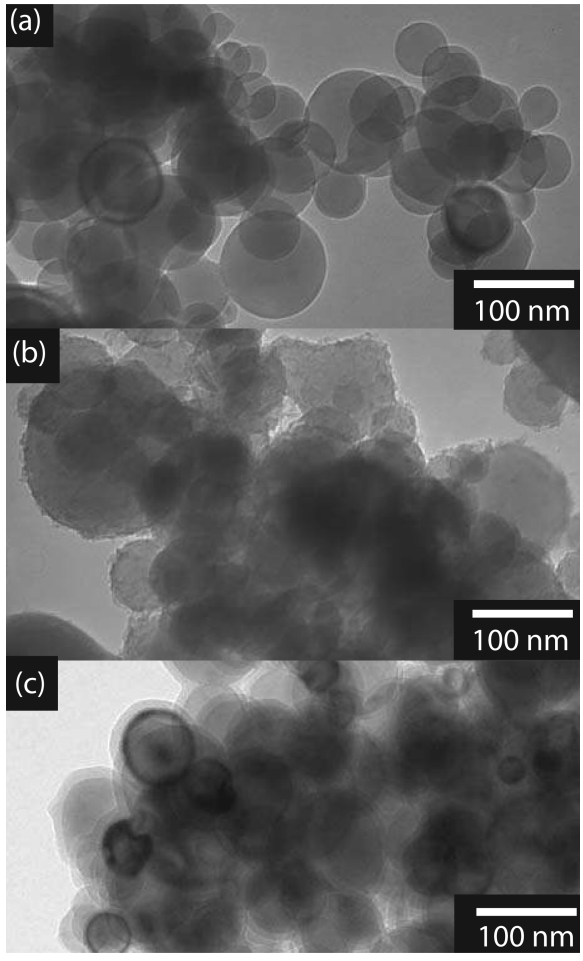

Figure 5. TEM micrographs of aluminum particles that were (a) transferred from a glovebox to a sealed container, (b) exposed to air and humidity, and (c) coated with perfluorodecalin (PFD) and were exposed to humidity and air.

dx.doi.org/10.1021/am5012707 | ACS Appl. Mater. Interfaces 2014, 6, 7942−7947

particles have retain their smooth spherical surface. Uncoated particles exposed to moisture show visible damage, develop a rough surface, and lose their spherical shape (see Figure 5b). PFD-coated particles show no visible damage after exposure and have the visual appearance of the sample stored in the glovebox (see Figure 5c). FESEM micrograms show similar results (see Figure S1 in the Supporting Information).

Energy-dispersive spectroscopy (EDS) provides direct evidence of oxidation of the metal (Figure 6). The spectrum

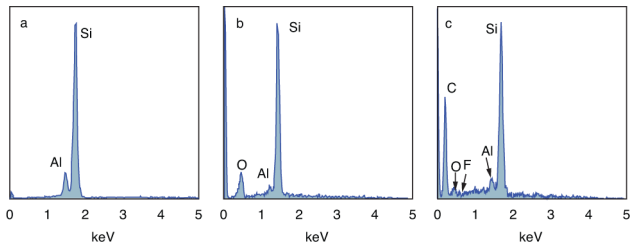

Figure 6. Energy-dispersive spectroscopy (EDS) graphs of aluminum nanoparticles (a) uncoated kept in glovebox, (b) uncoated exposed to air and humidity, and (c) coated with PFD plasma polymer exposed to air and humidity.

of the sample stored in the glovebox shows a strong peak from aluminum but no oxygen. Oxygen was detected in the uncoated sample that was exposed to air (Figure 6b). Trace oxygen was detected in the sample coated with PFD (Figure 6c). We note that the strong Si signal is due to the silicon wafer on which the particles were examined.

To measure the aluminum content of different samples, we performed TGA by heating in air. The sample was oxidized by slow heating in air and the amount of aluminum was calculated from the weight gain due to the formation of the oxide. Therefore, the method gives a direct measure of the aluminum content of the particles and provides a quantitative measure of the coating to provide passivation. Other possible gain weight due to oxinitride and aluminum nitride formation[42] may take place if self-ignition occurs.[43] This is avoided by a slow rate of heating. For these experiments, heating was done according to the following schedule: 20 °C/min, up until 350 °C; 5 °C/min, from 350 °C to 600 °C; followed by 20 °C/min, from 600 °C to 850 °C. The sample was kept at 850 °C for 4 h before cooling to room temperature to ensure that all of the aluminum has reacted. The TGA experiments were done three times and the results are reproducible within ±5% error.

Five samples were analyzed using this method: three coated samples after exposure to air (isopropyl alcohol (IPA), toluene, PFD), uncoated aluminum after exposure to air, and uncoated aluminum stored in the glovebox (control, no exposure to air beyond that during handling). The thermogravimetric profiles of these samples are shown in Figure 7. The first weight loss for all samples is observed immediately upon heating and is completed at <350 °C (~20 min). In this temperature range, the plasma coatings are thermally stable.[30,31] The initial weight loss is due to the evaporation of water and other volatile vapors. Notably, particles that were kept in glovebox were not exposed to air and humidity and show the smallest weight loss. Uncoated exposed particles show the maximum weight loss during this step (~20%). The samples coated with IPA, toluene, and PFD lose 8%, 4.2%, and 4% of their weight, respectively. All weights are normalized to the weight of the degassed sampled.

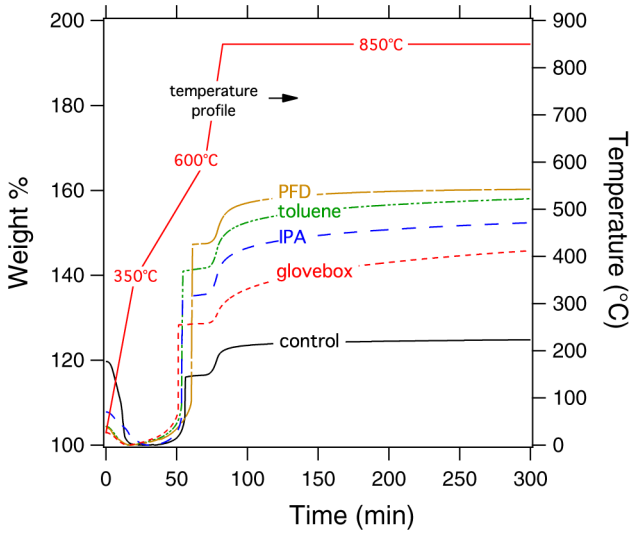

Figure 7. Thermogravimetric analysis (TGA) graph of coated and uncoated aluminum placed under 90% relative humidity for one month.

The next change in weight is an increase observed between 350°C to 500°C (~50 min) and is due to the oxidation of aluminum. A small weight loss is expected due to the decomposition of the coatings, but this is clearly overshadowed by the large weight gain due to the oxidation of aluminum. Near 500 °C, all the samples reach a plateau for almost 20 min, because of the buildup of an oxide layer that prevents further oxidation. Another weight gain is observed at near 650 °C. The melting point for 100-nm aluminum is reported to be 656 °C;[11] accordingly, this gain is attributed to the melting of the Al core, which facilitates further oxidation. By the end of the experiment (340 min) the weight gain practically levels off and reaches its maximum amount. The exposed uncoated sample shows a weight gain of only 20% weight. The weight gain of the coated particles are all higher. Coated particles with IPA, toluene, and PFD show weight increases of 52%, 58%, and 60%, respectively, indicating increasing degree of protection by the corresponding coatings.

Notably, all coated samples gained more weight than the uncoated sample stored in the glovebox. This result is surprising, because the uncoated sample kept under inert atmosphere is expected to register at least the same aluminum content as coated samples that were exposed to humidity. The weight gain of the glovebox sample is ~46% and agrees with similar published studies on bare aluminum nanoparticles.[44,45] The results suggest that the oxidation of the uncoated aluminum is not complete and that the coating contributes to more-complete oxidation and, thus, higher weight gain.[46] To investigate this possibility further, we studied these samples using DSC. This method measures the heat flow and temperature associated with phase transitions or reactions, as a function of temperature, as shown in Figure 8, and provides information about physical and chemical changes that involve endothermic or exothermic processes (see Figure S2 in the Supporting Information). The coating starts to degrade at ~250 °C, and the exothermic process due to C−C and C−F cross-linking is seen in Figure 8a as a small peak.[30] A sharp peak due to exothermic oxidation occurs at ~520°C for the uncoated aluminum sample, 541, 542, and 555 °C for toluene-coated, IPA-coated, and PFD-coated aluminum, respectively (see

dx.doi.org/10.1021/am5012707 | ACS Appl. Mater. Interfaces 2014, 6, 7942−7947

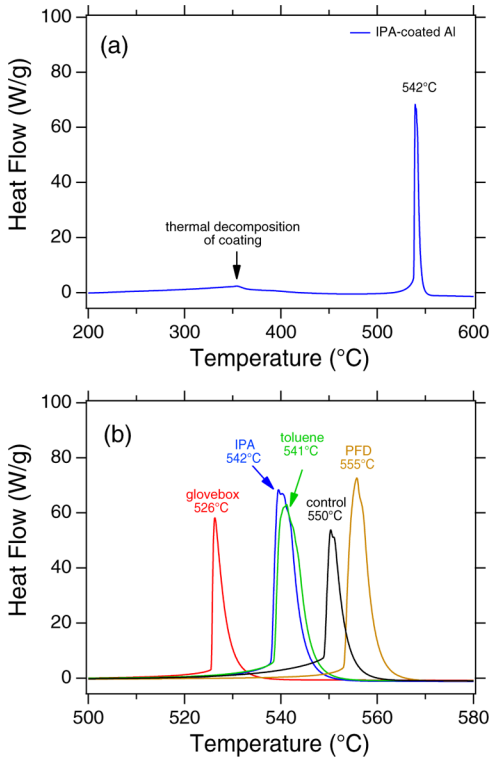

Figure 8. Differential scanning calorimetry (DSC) scans of samples after exposure at 85% relative humidity (PT) for a month: (a) complete thermogram for IPA-coated samples and (b) comparison of exothermic peaks due to oxidation of aluminum.

Figure 8b). The heat of reaction (ΔH) is determined by measuring the area of the DSC peak on a time basis, as reported in Table 1. The coated samples have a higher heat of combustion than the uncoated samples and are ranked in the following order: IPA < toluene < PFD, in agreement with the TGA results. The uncoated sample that was exposed to humidity has the lowest heat of combustion, and the one stored in the glovebox has the second lowest enthalpy, 10% lower that the poorest coating (IPA) and 44% lower than the best (PFD). The weight gain in TGA correlates fully with the measured enthalpies and suggests that the coatings indeed promote more-complete reaction. Others have reported similar effects.[47,48] Guo et al.[48] coated aluminum nanopowders with hydroxyl-terminated polybutadiene, stored the particles for 2 years, and reported a heat of combustion of 3.87 kJ/g, compared to 1.27 kJ/kg for untreated particles. These values are in general agreement with the results reported here. The advantage in the plasma process, compared to chemical treatments such as that of Guo et al.,[48] is that, in addition to the flexibility afforded by the choice of the precursor, we may control the thickness of the layer and thus optimize the final powder, with respect to the degree of passivation achieved, the amount of energy released, and the amount of coating that is added to the fuel.

Table 1. Enthalpy of Combustion for Coated and Uncoated Aluminum Particles

sample	exposure to humidity	ΔH (kJ/g)
uncoated aluminum	no[a]	3.12
uncoated aluminum (control)	yes	2.15
coated aluminum with IPA	yes	4.20
coated aluminum with toluene	yes	4.40
coated aluminum with PFD	yes	4.65

[a]Stored in glovebox.

4. CONCLUSIONS

We have developed a process to passivate aluminum nanoparticle surfaces via a dry state process. We produced 5-nm coatings on 80-nm aluminum nanoparticles by plasma deposition of isopropyl alcohol (IPA), toluene, and perfluorodecalin (PFD). The coatings provide excellent protection against contact with NaOH and against two month-long exposure to high humidity, and they preserve a higher amount of metallic aluminum, compared to samples stored in inert atmosphere for the same period of time. The materials are ranked in the following order: PFD > toluene > IPA. This order is observed with respect to the contact angle of water; the amount of metallic aluminum, as determined by TGA; and heat of reaction, as determined by DSC. Therefore, the performance of the coatings, with respect to passivation and energy release, correlates with the measured contact angle. This suggests that a hydrophobic interaction is important in building a barrier against humidity. This property can be fine-tuned by proper selection of the chemical precursor.

■ ASSOCIATED CONTENT

Supporting Information

FESEM images and DSC micrograms of uncoated and coated aluminum nanoparticles. This material is available free of charge via the Internet at http://pubs.acs.org.

■ AUTHOR INFORMATION

Corresponding Author

*Tel.: +1(814)863-2002. Fax: +1(814)865-7846. E-mail: matsoukas@engr.psu.edu.

Notes

The authors declare no competing financial interest.

■ ACKNOWLEDGMENTS

The authors gratefully acknowledge Dr. Kiarash Vakhshouri for his help with handling nanoparticles in glovebox. We also thank Mrs. Saba Lotfizadeh, Mrs. Julie Anderson, and Mrs. Angie Fan for their helpful advice and discussions. This material is based upon work supported by the National Science Foundation, under Grant No. CTS 1132220.

■ REFERENCES

(1) Pivkina, A.; Ulyanova, P.; Frolov, Y.; Zavyalov, S.; Schoonman, J. Nanomaterials for Heterogeneous Combustion. *Propellants, Explos., Pyrotech.* **2004**, *29*, 39−48.

(2) Zhi, J.; Shu-Fen, L. Research on the Combustion Properties of Propellants with Low Content of Nano Metal Powders. *Propellants, Explos., Pyrotech.* **2006**, 139−147.

(3) Malchi, J. Y.; Foley, T. J.; Yetter, R. A. Electrostatically Self-Assembled Nanocomposite Reactive Microspheres. *ACS Appl. Mater. Interfaces* **2009**, *1*, 2420−2423.

(4) Meda, L.; Marra, G.; Galfetti, L.; Severini, F.; De Luca, L. Nano-Aluminum as Energetic Material for Rocket Propellants. *Mater. Sci. Eng., C* **2007**, *27*, 1393−1396.

(5) Dreizin, E. L. Metal-based Reactive Nanomaterials. *Prog. Energy Combust. Sci.* **2009**, *35*, 141−167.

(6) Zhou, X.; Torabi, M.; Lu, J.; Shen, R.; Zhang, K. Nanostructured Energetic Composites: Synthesis, Ignition/Combustion Modeling, and Applications. *ACS Appl. Mater. Interfaces* **2014**, *6*, 3058−3074.

(7) Huang, Y.; Risha, G. A.; Yang, V.; Yetter, R. A. Effect of Particle Size on Combustion of Aluminum Particle Dust in Air. *Combust. Flame* **2009**, *156*, 5−13.
(8) Puri, P.; Yang, V. Effect of Particle Size on Melting of Aluminum at Nano Scales. *J. Phys. Chem. C* **2007**, *111*, 11776−11783.
(9) Morgan, A. B.; Wolf, J. D.; Guliants, E. A.; Fernando, K.; Lewis, W. K. Heat Release Measurements on Micron and Nano-Scale Aluminum Powders. *Thermochim. Acta* **2009**, *488*, 1−9.
(10) Foley, T. J.; Johnson, C. E.; Higa, K. T. Inhibition of Oxide Formation on Aluminum Nanoparticles by Transition Metal Coating. *Chem. Mater.* **2005**, *17*, 4086−4091.
(11) Lan, X. Z.; Tan, Z.-C.; Quan, S.; Yang, C. G. A Novel Gelling Method for Stabilization of Phase Change Material $Na_2HPO_4{\cdot}12H_2O$ with Sodium Alginate Grafted Sodium Acrylate. *Thermochim. Acta* **2007**, *463*, 18−20.
(12) Sanchez-Lopez, J.; Caballero, A.; Fernandez, A. Characterisation of Passivated Aluminium Nanopowders: An XPS and TEM/EELS Study. *J. Eur. Ceram. Soc.* **1998**, *18*, 1195−1200.
(13) Kravchenko, O.; Semenenko, K.; Bulychev, B.; Kalmykov, K. Activation of Aluminum Metal and its Reaction with Water. *J. Alloys Compd.* **2005**, *397*, 58−62.
(14) Chung, S. W.; Guliants, E. A.; Bunker, C. E.; Hammerstroem, D. W.; Deng, Y.; Burgers, M. A.; Jelliss, P. A.; Buckner, S. W. Capping and Passivation of Aluminum Nanoparticles Using Alkyl-Substituted Epoxides. *Langmuir* **2009**, *25*, 8883−8887.
(15) Dai, J.; Sullivan, D. M.; Bruening, M. L. Ultrathin, Layered Polyamide and Polyimide Coatings on Aluminum. *Ind. Eng. Chem. Res.* **2000**, 3528−3535.
(16) Jay, F.; Gauthier-Brunet, V.; Pailloux, F.; Mimault, J.; Bucher, S.; Dubois, S. Al-Coated Iron Particles: Synthesis, Characterization and Improvement of Oxidation Resistance. *Surf. Coat. Technol.* **2008**, *202*, 4302−4306.
(17) Gromov, A.; Ilyin, A.; Förter-Barth, U.; Teipel, U. Characterization of Aluminum Powders: II. Aluminum Nanopowders Passivated by Non-inert Coatings. *Propellants, Explos., Pyrotech.* **2006**, *31*, 401−409.
(18) Klepper, C.; Hazelton, R.; Yadlowsky, E.; Carlson, E.; Keitz, M.; Williams, J.; Zuhr, R.; Poker, D. Amorphous Boron Coatings Produced with Vacuum Arc Deposition Technology. *J. Vac. Sci. Technol., A* **2002**, *20*, 725−732.
(19) Yetter, R. A.; Risha, G. A.; Son, S. F. Metal Particle Combustion and Nanotechnology. *Proc. Combust. Inst.* **2009**, *32*, 1819−1838.
(20) Park, K.; Rai, A.; Zachariah, M. Characterizing the Coating and Size-resolved Oxidative Stability of Carbon-Coated Aluminum Nanoparticles by Single-Particle Mass-Spectrometry. *J. Nanopart. Res.* **2006**, *8*, 455−464.
(21) Jouet, R. J.; Warren, A. D.; Rosenberg, D. M.; Bellitto, V. J.; Park, K.; Zachariah, M. R. Surface Passivation of Bare Aluminum Nanoparticles using Perfluoroalkyl Carboxylic Acids. *Chem. Mater.* **2005**, *17*, 2987−2996.
(22) Jouet, R. J.; Carney, J. R.; Granholm, R. H.; Sandusky, H. W.; Warren, A. D. Preparation and Reactivity Analysis of Novel Perfluoroalkyl Coated Aluminium Nanocomposites. *Mater. Sci. Technol.* **2006**, *22*, 422−429.
(23) Kappagantula, K. S.; Pantoya, M. L.; Horn, J. Effect of Surface Coatings on Aluminum Fuel Particles toward Nanocomposite Combustion. *Surf. Coat. Technol.* **2013**, *237*, 456−459.
(24) Crouse, C. A.; Pierce, C. J.; Spowart, J. E. Influencing Solvent Miscibility and Aqueous Stability of Aluminum Nanoparticles through Surface Functionalization with Acrylic Monomers. *ACS Appl. Mater. Interfaces* **2010**, *2*, 2560−2569.
(25) Abadjieva, E.; van der Heijden, A. E.; Creyghton, Y. L.; van Ommen, J. R. Fluorocarbon Coatings Deposited on Micron-Sized Particles by Atmospheric PECVD. *Plasma Processes Polym.* **2012**, *9*, 217−224.
(26) Tran, N. D.; Dutta, N. K.; Choudhury, N. R. Plasma-Polymerized Perfluoro(methylcyclohexane) Coating on Ethylene Propylene Diene Elastomer Surface: Effect of Plasma Processing Condition on the Deposition Kinetics, Morphology and Surface Energy of the Film. *Thin Solid Films* **2005**, *491*, 123−132.
(27) Woodward, I.; Schofield, W. C. E.; Roucoules, V.; Badyal, J. P. S. Super-hydrophobic Surfaces Produced by Plasma Fluorination of Polybutadiene Films. *Langmuir* **2003**, *19*, 3432−3438.
(28) Kim, J.-H.; Liu, G.; Kim, S. H. Deposition of Stable Hydrophobic Coatings with In-line CH_4 Atmospheric RF Plasma. *J. Mater. Chem.* **2006**, *16*, 977−981.
(29) Kwok, Q. S.; Fouchard, R. C.; Turcotte, A.-M.; Lightfoot, P. D.; Bowes, R.; Jones, D. E. Characterization of Aluminum Nanopowder Compositions. *Propellants, Explos., Pyrotech.* **2002**, *27*, 229−240.
(30) Shahravan, A.; Matsoukas, T. Encapsulation and Controlled Release from Core−Shell Nanoparticles Fabricated by Plasma Polymerization. *J. Nanopart. Res.* **2012**, *14*, 1−11.
(31) Shahravan, A.; Yelamarty, S.; Matsoukas, T. Microbubble Formation from Plasma Polymers. *J. Phys. Chem. B* **2012**, *116*, 11737−11743.
(32) Mishra, D. *Fundamentals of Combustion*; PHI Learning Pvt. Ltd.: Delhi, India, 2008.
(33) Koch, E.-C. Metal/fluorocarbon Pyrolants: V. Theoretical Evaluation of the Combustion Performance of Metal/Fluorocarbon Pyrolants Based on Strained Fluorocarbons. *Propellants, Explos., Pyrotech.* **2004**, *29*, 9−18.
(34) Horn, J. M.; Lightstone, J.; Carney, J.; Jouet, J. Preparation and Characterization of Functionalized Aluminum Nanoparticles. *AIP Conf. Proc.* **2012**, *1426*, 607−610.
(35) Dubois, C.; Lafleur, P. G.; Roy, C.; Brousseau, P.; Stowe, R. A. Polymer-Grafted Metal Nanoparticles for Fuel Applications. *J. Propuls. Power* **2007**, *23*, 651−658.
(36) Cao, J.; T, M. Nanowire Coating by Plasma Processing. *IEEE Trans. Plasma Sci.* **2005**, *33*, 829−833.
(37) Cao, J.; Matsoukas, T. Synthesis of Hollow Nanoparticles by Plasma Polymerization. *J. Nanopart. Res.* **2004**, *6*, 447−455.
(38) Cao, J.; Matsoukas, T. Nanoparticles and Nanocomposites in RF Plasma. *Mater. Res. Soc. Symp.* **2001**, *635*, c.4.12.1−c.4.12.6.
(39) Cao, J.; Matsoukas, T. Deposition Kinetics on Particles in a Dusty Plasma Reactor. *J. Appl. Phys.* **2002**, *92*, 2916−2922.
(40) Matsoukas, T.; Cao, J. Film Deposition on Particles Trapped in the Sheath of Reactive Dusty Plasma: Effect of Size Distribution. *IEEE Trans. Plasma Sci.* **2004**, *32*, 699−703.
(41) Shahravan, A.; Desai, T.; Matsoukas, T. Controlled Manipulation of Wetting Characteristics of Nanoparticles with Dry-Based Plasma Polymerization Method. *Appl. Phys. Lett.* **2012**, *101*, 251603.
(42) Nakao, W.; Fukuyama, H.; Nagata, K. Gibbs Energy Change of Carbothermal Nitridation Reaction of Al_2O_3 to Form AlN and Reassessment of Thermochemical Properties of AlN. *J. Am. Ceram. Soc.* **2002**, *4*, 889−896.
(43) Repkin, Y. D.; Samsonov, G. Formation of Aluminum Nitride by Nitriding Aluminum Powder. *Powder Metall. Met. Ceram.* **1963**, *2*, 394−400.
(44) Levitas, V. I.; Pantoya, M. L.; Chauhan, G.; Rivero, I. Effect of the Alumina Shell on the Melting Temperature Depression for Aluminum Nanoparticles. *J. Phys. Chem. C* **2009**, *113*, 14088−14096.
(45) Trunov, M. A.; Umbrajkar, S. M.; Schoenitz, M.; Mang, J. T.; Dreizin, E. L. Oxidation and Melting of Aluminum Nanopowders. *J. Phys. Chem. B* **2006**, *110*, 13094−13099.
(46) Good, W. D.; Smith, N. K. Enthalpies of Combustion of Toluene, Benzene, Cyclohexane, Cyclohexene, Methylcyclopentane, 1-Methylcyclopentene, and *n*-Hexane. *J. Chem. Eng. Data* **1969**, *14*, 102−106.
(47) Zhou, X.; Xu, D.; Zhang, Q.; Lu, J.; Zhang, K. Facile Green In Situ Synthesis of Mg/CuO Core/Shell Nanoenergetic Arrays with a Superior Heat-Release Property and Long-Term Storage Stability. *ACS Appl. Mater. Interfaces* **2013**, *5*, 7641−7646.
(48) Guo, L.; Song, W.; Hu, M.; Xie, C.; Chen, X. Preparation and Reactivity of Aluminum Nanopowders Coated by Hydroxyl-Terminated Polybutadiene (HTPB). *Appl. Surf. Sci.* **2008**, *254*, 2413−2417.